Cell

Spatiotemporal Coupling of cAMP Transporter to CFTR Chloride Channel Function in the Gut Epithelia

Chunying Li,[1] Partha C. Krishnamurthy,[2] Himabindu Penmatsa,[1] Kevin L. Marrs,[1] Xue Qing Wang,[3] Manuela Zaccolo,[4] Kees Jalink,[5] Min Li,[6] Deborah J. Nelson,[3] John D. Schuetz,[2] and Anjaparavanda P. Naren[1,*]
[1]Department of Physiology, The University of Tennessee Health Science Center, 894 Union Avenue, 420 Nash, Memphis, TN 38163, USA
[2]Department of Pharmaceutical Sciences, St. Jude Children's Research Hospital, 332 North Lauderdale Street, Memphis, TN 38105, USA
[3]Department of Neurobiology, Pharmacology, and Physiology, The University of Chicago, 947 East 58th Street, MC 0926, Chicago, IL 60637, USA
[4]Dulbecco Telethon Institute, Venetian Institute of Molecular Medicine, Via Orus 2, 35124, Padva, Padova, Italy
[5]Division of Cell Biology, The Netherlands Cancer Institute, Plesmanlaan 121, 1066CX Amsterdam, The Netherlands
[6]Department of Neuroscience, The Johns Hopkins University School of Medicine, 733 North Broadway, Baltimore, MD 21205, USA
*Correspondence: anaren@utmem.edu
DOI 10.1016/j.cell.2007.09.037

SUMMARY

Cystic fibrosis transmembrane conductance regulator (CFTR) is a cAMP-regulated chloride channel localized at apical cell membranes and exists in macromolecular complexes with a variety of signaling and transporter molecules. Here, we report that the multidrug resistance protein 4 (MRP4), a cAMP transporter, functionally and physically associates with CFTR. Adenosine-stimulated CFTR-mediated chloride currents are potentiated by MRP4 inhibition, and this potentiation is directly coupled to attenuated cAMP efflux through the apical cAMP transporter. CFTR single-channel recordings and FRET-based intracellular cAMP dynamics suggest that a compartmentalized coupling of cAMP transporter and CFTR occurs via the PDZ scaffolding protein, PDZK1, forming a macromolecular complex at apical surfaces of gut epithelia. Disrupting this complex abrogates the functional coupling of cAMP transporter activity to CFTR function. *Mrp4* knockout mice are more prone to CFTR-mediated secretory diarrhea. Our findings have important implications for disorders such as inflammatory bowel disease and secretory diarrhea.

INTRODUCTION

The cyclic nucleotides (e.g., cAMP) are important second messengers involved in the cellular responses to a wide variety of signals in every living cell. In epithelial cells lining the gut, kidney, and lung, cAMP also plays key roles in the extracellular regulation of fluid homeostasis (Jackson and Raghvendra, 2004). Tight regulation of intracellular cAMP levels is critical, because excessive cAMP production within cells leads to overstimulation of certain secretory events, dysregulation of cell function, or even cell toxicity. Increased intracellular cAMP is restored to basal levels via hydrolysis into 5′-AMP by phosphodiesterases (PDEs) (Jackson and Raghvendra, 2004). Recently, the molecular identity of a cAMP efflux transporter has been discovered. MRP4 (ABCC4) is a member of the ATP-binding cassette (ABC) transporter superfamily, whose gene products are capable of transporting substrates from the inner membrane leaflet to the outer membrane leaflet (Dean et al., 2001). MRP4 has been shown to function as a high-affinity efflux pump for cAMP (Chen et al., 2001; van Aubel et al., 2002; Wielinga et al., 2003), is expressed in epithelial cells lining lung, kidney, intestine, etc., and is localized on both the apical membranes (van Aubel et al., 2002) and basolateral membranes (Lai and Tan, 2002) of polarized cells.

The concept of spatially restricted and tightly modulated compartmentalization of cAMP signaling events was formulated over 20 years ago (reviewed in Steinberg and Brunton, 2001; Cooper, 2005). It is well documented that cAMP signaling specificity relies substantially on the organization of macromolecular signaling complexes that effectively assemble multiple proteins (from receptors to targets) into three-dimensional arrays at subcellular locations, and that proximity of receptors to their ultimate targets guarantees response velocity and signaling specificity (Davare et al., 2001; Huang et al., 2001; Naren et al., 2003; Li et al., 2005). The assembly of this signaling complex ensures specific and rapid signaling from the receptor to the channel. Stimulation of β_2 adrenergic receptors (β_2ARs) in airway epithelial cells also activates chloride transport mediated by cystic fibrosis transmembrane

conductance regulator (CFTR), the product of the gene mutated in patients with cystic fibrosis (Li and Naren, 2005). Regulation of the CFTR Cl^- channel is accomplished through activation of this apical surface receptor that couples to adenylate cyclase (AC) and raises cellular cAMP. Huang and colleagues reported that signaling elements compartmentalized in apical compartments that activate CFTR in polarized lung epithelial cells (Huang et al., 2001). They observed that maximal stimulation of CFTR-mediated Cl^- secretion by adenosine, a ligand for A_{2b} adenosine receptors (A_{2b}ARs) that couple to membrane-bound AC, was accompanied by no measurable change in total cellular cAMP, signifying highly localized regulation of CFTR by A_{2b}ARs in the apical cell membrane (Huang et al., 2001).

The functional significance of the macromolecular complex containing CFTR and its interacting partners in subcellular compartments was reconfirmed (Li et al., 2005). Most recently, we demonstrated that a type 2 lysophosphatidic acid (LPA) receptor forms a macromolecular complex with CFTR, a process mediated through a PDZ scaffolding protein (NHERF2) at the apical surfaces of gut epithelial cells (Li et al., 2005). The assembly of this multiprotein complex forms the basis for the functional coupling between LPA signaling and CFTR-mediated chloride transport. In the present study, we observed a previously unidentified functional coupling of a cAMP efflux transporter (MRP4) to CFTR activity that is physically mediated through PDZK1/CAP70 scaffolding protein (Wang et al., 2000) in a spatially segregated microdomain; this interaction has important implications for diseases such as inflammatory bowel disease and secretory diarrhea.

RESULTS

Inhibition of a cAMP Transporter, MRP4, Potentiates the Function of the Colocalized CFTR Cl^- Channel at the Apical Surface of Gut Epithelial Cells

CFTR is localized at the apical membrane of epithelial cells lining the gut (Li and Naren, 2005). The functional activity of this Cl^- channel is regulated by PKA after a rise in the local concentration of cAMP. We hypothesized that inhibition of the plasma membrane cAMP efflux transporter MRP4 would enhance the cAMP signal and thus magnify CFTR function. In this study, gut epithelial cells were permeabilized at the basolateral surface with α-toxin derived from *Staphylococcus aureus*; the cells were then pretreated with MK571, a potent MRP4 inhibitor (Reid et al., 2003). α-toxin forms pores that are permeable to molecules < 5000 Da, therefore effectively removing the basolateral membrane as a barrier to cAMP without affecting the functional integrity of the apical membrane (Reddy and Quinton, 1996). The cell membrane-impermeable agonist (cAMP) was added to the permeabilized surface of polarized gut epithelial cell monolayers to elicit CFTR-mediated short-circuit currents (I_{sc}). In basolateral-permeabilized cells pretreated with MK571, a low dose of cAMP (10 μM) elicited a near-maximal CFTR-mediated I_{sc}, which was not boosted further by a higher dose of cAMP (50 μM) (Figure 1A, top). Whereas in untreated (or vehicle-treated) cells, 10 μM cAMP induced only a very small I_{sc} response (only 30%–40% magnitude of the MK571-treated cells), the currents can be further increased to a maximal level by higher dose of cAMP (50 μM) (Figure 1A, bottom). However, at a dose of 20 μM cAMP, maximal CFTR-dependent I_{sc} responses were observed both in the presence and absence of MK571 (Figure 1B). The I_{sc} potentiated by MK571 in basolateral-permeabilized gut epithelial cells were inhibited by various CFTR inhibitors (glybenclamide, as in Figure 1A; a CFTR-specific inhibitor, $CFTR_{inh}$-172, as in Figure S1A in Supplemental Data available with this article online). Experiments were also performed to demonstrate that cAMP did not activate CFTR in nonpermeabilized cells when added at either apical or basolateral surfaces (Figure S2A, bottom). Also, in cells permeabilized at the basolateral side, cAMP did not activate CFTR from the apical surface (Figure S2A, top).

We consistently observed that, in MK571-pretreated cells, the cAMP-activated state of the CFTR Cl^- channel is sustained for a relatively longer period of time compared to untreated cells, i.e., the deactivation of the channel was relatively slower in the presence of MK571 (Figures 1A, 1B, and S1A). This potentiation (enhancement) of CFTR function in response to exogenous cAMP by the MRP4 inhibitor (MK571) raises the possibility that attenuated or blocked, MRP4-mediated, apical cAMP efflux by MK571 may help accumulate higher levels of the second messenger in close proximity to the CFTR Cl^- channel, thus resulting in increased CFTR Cl^- currents, as opposed to what is seen with the untreated control.

Using an MRP4-specific antibody, we detected MRP4 expression by immunoblotting in the crude membranes prepared from gut epithelial cells (HT29-CL19A and T84 cells) (Figure 1C). Immunoreactivity for MRP4 was not observed in the cytosol (Figure 1C). Immunofluorescent confocal microscopy demonstrated that MRP4 is localized to both the apical and basolateral membranes of HT29-CL19A cells (Figure 1D, left), with a higher abundance on the apical plasma membrane, where it colocalizes partially with CFTR (Figure 1D, right).

cAMP Transporter Function at the Apical Plasma Membrane of Gut Epithelial Cells Is Inhibited by MK571

Given that MRP4 is localized in part at the apical membranes of epithelial cells, the unidirectional transport of etheno-cAMP (a fluorescent analog of cAMP) and [^{3}H]cAMP across the apical membranes of basolateral-permeabilized polarized gut epithelial cells was monitored. Etheno-cAMP, like cAMP, is cell impermeant and induced CFTR-mediated Cl^- currents in basolaterally permeabilized epithelial cells only (Figure S3A, bottom). As MK571 itself has significant autofluorescence when excited at the same wavelength as etheno-cAMP (ex315 nm/em420 nm), we used an MRP4 substrate, 9-(2-phosphonyl methoxyethyl) adenine (PMEA), which

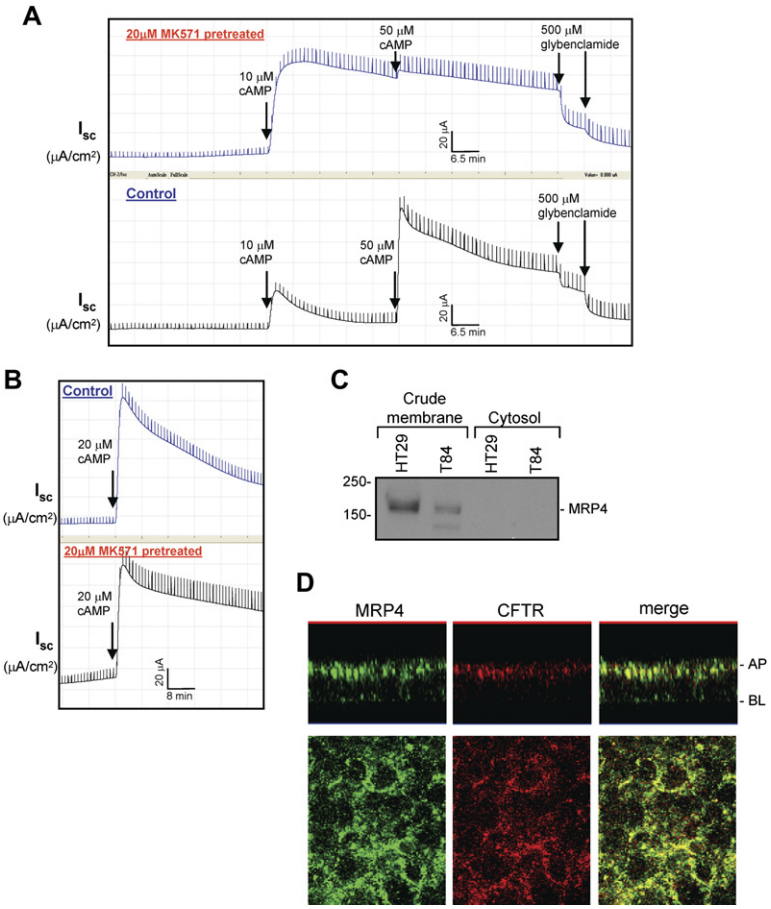

Figure 1. The MRP4 Inhibitor MK571 Potentiates CFTR-Mediated Short-Circuit Currents

(A and B) Representative traces of CFTR-mediated short-circuit currents (I_{sc}) in response to cAMP in basolateral-permeabilized HT29-CL19A cells. Basolateral membranes of the polarized cells were permeabilized with 100 μg/ml α-toxin for 30 min. Cells were pretreated with 20 μM MK571 on both sides before cAMP was added to the basolateral side. A CFTR inhibitor, glybenclamide, was added to the apical side at the end of the experiment.

(C) MRP4 expression in crude plasma membrane prepared from colonic epithelial cells (HT29-CL19A cells and T84 cells).

(D) Localization of MRP4 and CFTR in polarized HT29-CL19A cells by confocal fluorescence microscopy. Top, x-z axis images; bottom, x-y axis images. AP, apical membrane; BL, basolateral membrane.

is a stable, monophosphorylated nucleotide analog (Schuetz et al., 1999), to compete with etheno-cAMP for MRP4-mediated efflux across the apical membrane of polarized epithelial cells. As illustrated in Figure S3B, PMEA significantly decreased etheno-cAMP transport across the apical membrane of HT29-CL19A cells. The inhibitory effect of PMEA on etheno-cAMP efflux demonstrated a dose dependence (Figure S3B). Likewise, both MK571 and PMEA dose-dependently decreased the unidirectional transport of [^{3}H]cAMP from the basolateral chamber into the apical chamber through the apical membrane MRP4 transporter in HT29-CL19A cells (Figures 2A and 2B). These data clearly show that competitive interactions with an MRP4 inhibitor (MK571) or substrate (PMEA)

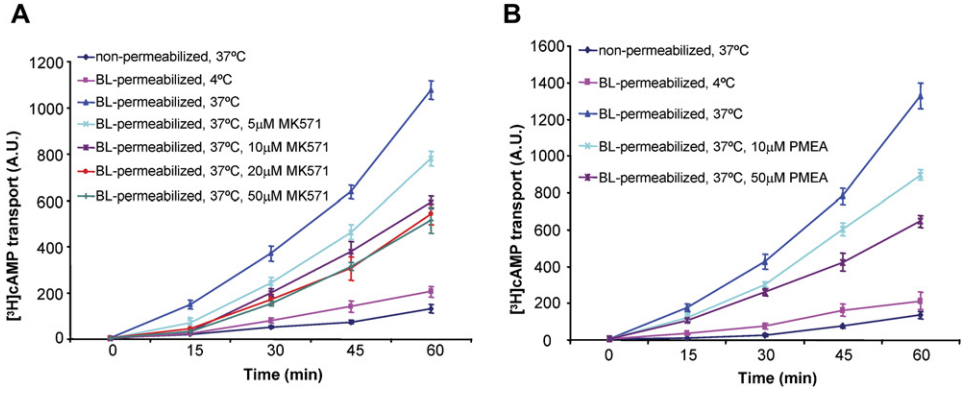

Figure 2. cAMP Transport across the Apical Plasma Membrane Is Inhibited by the MRP4 Inhibitor and Substrate

(A and B) Unidirectional transport of [^{3}H]cAMP by the apical MRP4 in basolateral-permeabilized HT29-CL19A cells pretreated with (A) the MRP4 inhibitor MK571 or (B) the MRP4 substrate PMEA. A.U. = arbitrary units. Data represent the mean ± SEM (n = 4).

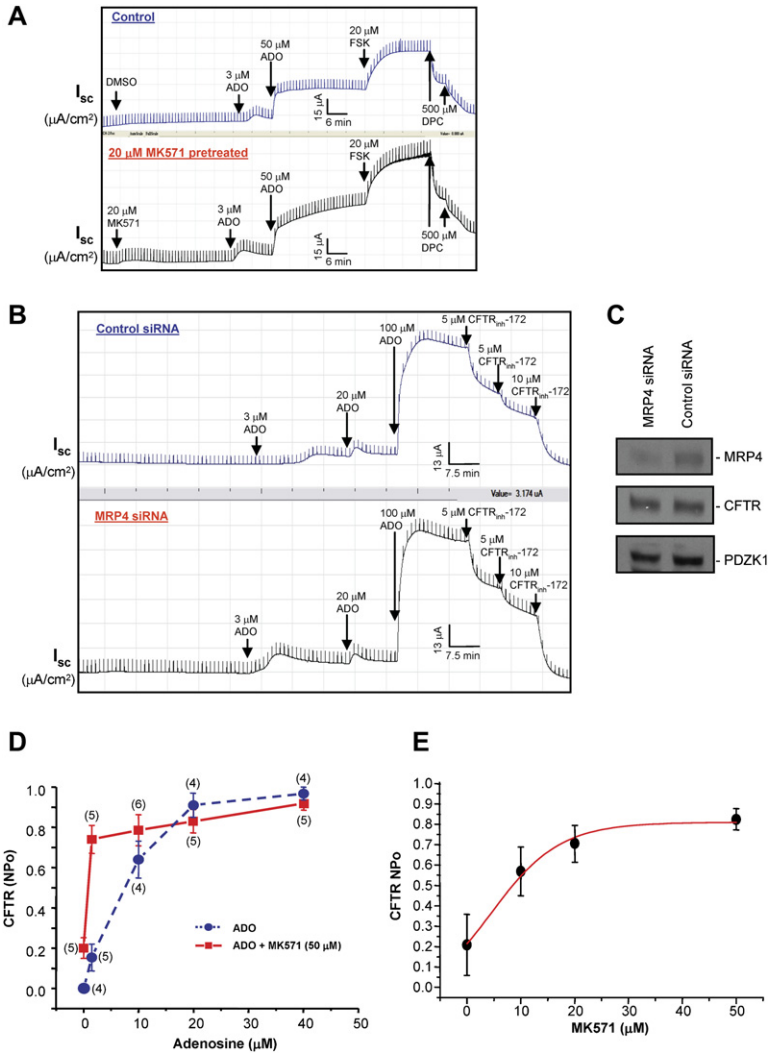

Figure 3. MRP4 Inhibition Potentiates CFTR-Mediated Cl^- Currents in a Compartmentalized Manner

(A) CFTR-mediated short-circuit currents (I_{sc}) in response to adenosine (ADO) and forskolin (FSK) in MK571-pretreated HT29-CL19A cells (bottom) or vehicle (DMSO)-treated cells (top). ADO, FSK, and a CFTR inhibitor, DPC, were added to the apical side.

(B) CFTR-mediated I_{sc} in response to ADO in MRP4 siRNA-transfected HT29-CL19A cells (bottom) or control siRNA-transfected cells (top). A CFTR-specific inhibitor, $CFTR_{inh}$-172, was added to the apical side.

(C) The protein levels of MRP4, CFTR, and PDZK1 in the cells from (B) were assessed by western blot with corresponding antibodies as described in Supplemental Experimental Procedures.

(D) Cell-attached single-channel recordings of CFTR currents in vehicle-treated (circle) or MK571-pretreated (square) HT29-CL19A cells in response to ADO. NPo: open-state probability of the channel. Numbers in parentheses indicate the number of patches for each condition. Error bars show SEM.

(E) Dose-dependence curve of CFTR NPo at different concentrations of MK571 when cells were activated by 1.5 μM ADO in HT29-CL19A cells. Data represent the mean ± SEM (n = 4–6).

reduce cAMP efflux across the intact apical MRP4 transporter when the basolateral membrane barrier to cAMP is removed in polarized epithelial cells.

Inhibition of cAMP Transporter Activity Potentiates CFTR Function in a Compartmentalized Fashion

cAMP-elevating ligand adenosine (ADO) has been reported to stimulate CFTR-mediated Cl^- currents in a compartmentalized manner at the apical cell membrane of polarized epithelial cells (Huang et al., 2001). ADO is produced at almost 1 μM in unstressed tissue, whereas in inflamed or ischemic tissues it can be as high as 100 μM (Hasko and Cronstein, 2004). Under conditions of inflammation (e.g., inflammatory bowel disease), ADO is generated at sites of tissue stress and injury and secreted into the gut, which would eventually activate CFTR (by acting on certain ARs and causing increased cAMP production [see Li et al., 2005]) and lead to increased chloride and fluid secretion into the gut lumen (Barrett and Keely, 2000). Because inhibition of MRP4 by MK571 reduced the cAMP efflux via apical MRP4 transporter (Figure 2A), and also potentiated CFTR Cl^- channel function in response to exogenous cAMP stimulation in basolateral-permeabilized epithelial cells (Figures 1A and S1A), we sought to monitor the effect of MK571 on CFTR-mediated I_{sc} across intact (nonpermeabilized), polarized gut epithelial cell monolayers in response to ADO. MK571 potentiated CFTR channel function in response to ADO stimulation, and the potentiating effect of MK571 on CFTR-mediated Cl^- currents was more prominent when CFTR was activated with a lower concentration of ADO (at 3 μM ADO, ~2-fold I_{sc} for MK571-treated cells compared to the control; at 50 μM ADO, ~1.4-fold I_{sc} for MK571-treated cells compared to the control) (Figures 3A and Figure S1B). However, MK571 failed to significantly potentiate the channel function when CFTR was maximally stimulated with a relatively higher dose of ADO (100 μM) (Figure S2B) or 20 μM forskolin (FSK), the adenylyl cyclase stimulator (Figure 3A), which causes a global increase of the intracellular cAMP level (Li et al., 2005). It is worthy to note that MK571 itself

can induce a very small I_{sc} (~3–5 μA/cm^2) even in the absence of ADO stimulation (Figure 3A, bottom).

To test the hypothesis that the potentiating effect of MK571 on CFTR-mediated Cl^- currents derives from the inhibitory effect of MK571 on MRP4 function, we used MRP4 siRNA oligonucleotides to specifically knock down the endogenous MRP4 protein amount, then monitored the CFTR-mediated Cl^- currents in response to ADO stimulation. MRP4 siRNA significantly enhanced the ADO-stimulated I_{sc} in HT29-CL19A epithelial cells compared to control siRNA, with the enhancing effect occurring at the lower dose (3 μM) of ADO stimulation (Figure 3B; Figure S1C). When CFTR was stimulated with a relatively higher dose of ADO (20–100 μM), there was no difference in CFTR-mediated I_{sc} between control cells and MRP4 knockdown cells (Figure 3B). The specificity of MRP4 siRNA was also checked to show that MRP4 siRNA did not affect the endogenous CFTR or PDZK1 protein levels (Figure 3C). The Cl^- currents potentiated by MK571 or MRP4 siRNA in nonpermeabilized gut epithelial cells were inhibited by a CFTR blocker, DPC (Figure 3A), and by the CFTR-specific inhibitor, $CFTR_{inh}$-172 (Figure 3B; Figures S1B and S1C), suggesting that the enhanced I_{sc} by MK571 or MRP4 siRNA were mediated through the CFTR Cl^- channel.

Cell-attached, CFTR single-channel recordings confirmed that MK571 leads to compartmentalized accumulation of cAMP at or near the plasma membrane. Varying concentrations (0–40 μM) of ADO were applied in the patch pipette either to evoke a localized generation of intracellular cAMP (<20 μM ADO) or to elicit a significantly higher level (>20 μM ADO) of the second messenger, which might activate CFTR function submaximally or maximally (Huang et al., 2001; Li et al., 2005). In gut epithelial cells pretreated with MK571, the stimulatory effect of ADO on the CFTR single-channel activity (channel open-state probability, NPo) was compared with that in the untreated cells (Figures 3D and S4). The single-channel activity was significantly increased at concentrations of 1.5–10 μM ADO in the presence of MK571 compared to the control (Figures 3D and S4). In contrast, at doses of ADO > 20 μM in the pipette (leading to a significantly higher increase of intracellular cAMP, which might activate CFTR function submaximally or maximally), MK571 no longer potentiated channel function. It is to be noted that the NPo of CFTR Cl^- channels was significantly higher in MK571-pretreated cells (NPo = 0.2) compared to untreated cells (NPo = 0), even in the absence of ADO stimulation (Figure 3D), which is consistent with the above-described observation that MK571 itself can induce a very small I_{sc} (~3–5 μA/cm^2), even in the absence of ADO stimulation (Figure 3A, bottom). This suggests that MK571 itself, by inhibiting MRP4, might restrain a certain amount of localized cAMP within a microdomain, which is enough to elicit a certain level of CFTR stimulation. The potentiation of CFTR function by MK571 also demonstrates a dose dependence; the linear increase range falls within 0–30 μM of MK571 used when the CFTR channel was stimulated in a localized pattern by only 1.5 μM ADO (Figure 3E). MK571 potentiates CFTR activity with concentrations as low as 10 μM, and it is maximized by 30 μM (Figure 3E). All of the above-described data suggest that MK571 potentiates CFTR-mediated Cl^- currents in a locally restricted manner when CFTR is not maximally activated.

To further characterize the cAMP location after inhibition of the cAMP transporter, we used a FRET-based cAMP indicator, CFP-EPAC-YFP (Ponsioen et al., 2004), to monitor the effect of MK571 on intracellular cAMP signaling and dynamics in response to cAMP-elevating agents (such as ADO or FSK) in live cells. This highly sensitive, unimolecular, fluorescent indicator for cAMP can display significant FRET change, which rapidly diminishes after a rise in intracellular cAMP and increases again in response to a fall in cAMP, making it an ideal fluorescent probe for monitoring cAMP dynamics in living cells (Ponsioen et al., 2004). In gut epithelial cells (T84) expressing the CFP-EPAC-YFP indicator for intracellular cAMP, FSK, the potent cAMP-raising agent, evoked, on average, a 29% increase of the CFP/FRET emission ratio (CFP/FRET emission ratio corresponding to intracellular cAMP signals; also see Supplemental Experimental Procedures for details) (Figure S5), which indicates a global increase of intracellular cAMP. This is consistent with the observations of Ponsioen et al. (2004). As shown in Figure 4A (top), MK571 itself also induced a small but substantial increase of the CFP/FRET emission ratio (~8%; indicating increased cAMP level), as observed from I_{sc} measurements (Figure 3A, bottom) and CFTR single-channel recordings (Figure 3D). Interestingly, the most prominent increase of the CFP/FRET emission ratio, after blocking the cAMP efflux transporter MRP4, occurred at the edge area of the cells, which indicates a localized (spatially restricted) cAMP accumulation near the plasma membrane (i.e., subcellular cAMP heterogeneity) (Figure 4A, top).

As expected, ADO elicited a dose-dependent increase of the CFP/FRET emission ratio. A lower dose of ADO (2 μM) elicited a smaller increase of the ratio (~7%; Figure 4A, middle, and Figures 4B and 4E) compared to a higher dose of ADO (100 μM), with a much higher ratio was observed (~24%; Figure 4C, top, and Figures 4D and 4E). Interestingly, MK571 led to a significant increase of the cAMP level in addition to the cAMP increase caused by a lower dose of ADO (2 μM) (from ~7% to ~17%; Figure 4A, middle and bottom, Figures 4B and 4E). However, MK571 failed to execute any significant increase of cAMP on top of the one caused by a higher dose of ADO (100 μM) (from ~24% to ~25%; Figures 4C–4E). These results reveal a transition from compartmentalized cAMP elevation (Figure 4A) to a global increase of intracellular cAMP (Figure 4C; indicated by the uniform increase of the emission ratio in the entire cytoplasm), which is similar to the effect seen with 20 μM FSK (from ~28.8% to ~29%; Figures 4E and S5). This finding is consistent with the data from the above-described functional studies, the I_{sc} measurements (Figures 1A, 1B, and 3A), and cell-attached single-channel recordings (Figure 3D). These results imply that the

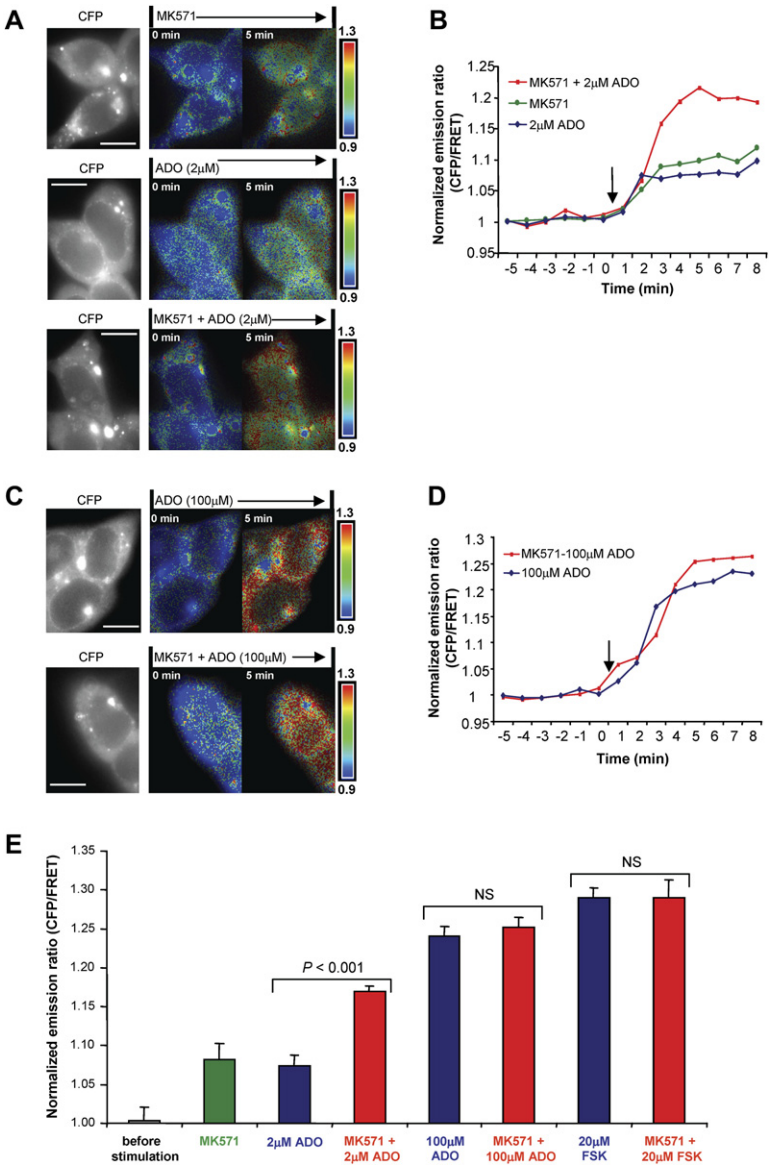

Figure 4. MRP4 Inhibition Enhances Intracellular cAMP Signals

(A) The monochrome CFP image showing the cytosolic distribution of the fluorescent EPAC probe in T84 cells transfected with CFP-EPAC-YFP, and representative pseudocolor images of the CFP/FRET emission ratio before (time = 0 min) and after the addition of 20 μM MK571 and/or 2 μM ADO (time = 5 min). The images in each panel were captured from the same field of view. The color bar shows the magnitude of the emission ratio. The scale bar is 10 μm.

(B) Kinetics of cAMP changes (represented by the normalized CFP/FRET emission ratio) recorded in the cells shown in (A). The arrow indicates the addition of the reagents.

(C) CFP image and representative pseudocolored CFP/FRET ratio images before (time = 0 min) and after the addition of 20 μM MK571 and/or 100 μM ADO (time = 5 min). The probe was excluded from the nuclear compartments, although, in these nonconfocal images, a signal emanating from above and below the nucleus gives the appearance of a nuclear ratio change. The scale bar is 10 μm.

(D) Kinetics of cAMP changes (normalized CFP/FRET emission ratio) recorded in the cells shown in (C). The arrow indicates the addition of the reagents.

(E) The summary of all of the experiments performed in the same conditions as in (A)–(D) and in Figure S5. Data represent the mean ± SEM (n = 4–6). NS, no significance.

increased cAMP accumulation through inhibiting cAMP efflux (via MRP4 transporter) demonstrates the biggest magnitude only when it is happening in a compartmentalized, spatially restricted microdomain near the plasma membrane, suggesting a spatial cAMP heterogeneity within a single cell.

Inhibition of a cAMP Transporter In Vivo Induces Secretory Diarrhea in Mice

CFTR plays a critical role in cholera toxin (CTX)-induced intestinal fluid secretion (secretory diarrhea) (Clarke et al., 1992; Li et al., 2005). Given that MK571 inhibits MRP4 activity and thus cAMP transport, leading to CFTR Cl^- channel activation as demonstrated in the above-described studies, we therefore hypothesized that inhibition of MRP4 can induce secretory diarrhea in mice. To test this hypothesis, the effect of MK571 on CTX-induced, CFTR-mediated intestinal fluid secretion was monitored in a closed-loop model of secretory diarrhea in wild-type and *Mrp4* knockout mice. CTX (0.5 μg) elicited a fluid accumulation in ligated ileal loops of both wild-type and *Mrp4* knockout mice (Figures 5A and 5B). MK571 treatment significantly increased the fluid accumulation in the toxin-treated intestinal loops in wild-type mice (Figure 5A), but failed to do so in *Mrp4* knockout mice (Figure 5B). Interestingly, we observed that the PBS control loop in *Mrp4* knockout mice, compared to wild-type mice, demonstrated a slightly, also significantly, higher level of fluid secretion (Figure 5C; ~24%, $p < 0.05$, n = 10–11). In addition, a CTX-injected loop in *Mrp4* knockout mice also demonstrated a significantly higher level of fluid accumulation compared to the loop in the wild-type mice (Figure 5C; ~27%, $p < 0.01$, n = 12–13). The MK571-potentiated, toxin-induced intestinal fluid

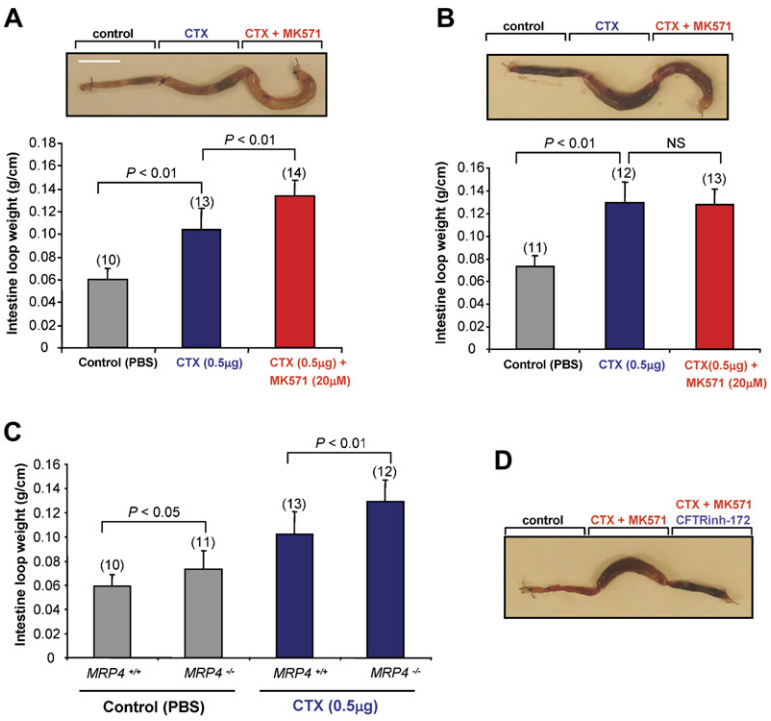

Figure 5. MRP4-Deficient Mice Are More Prone to CFTR-Mediated Secretory Diarrhea

(A and B) Representative mouse ileal loops 6 hr after luminal injection with CTX (0.5 μg) with or without MK571 (20 μM) (picture) in (A) wild-type mice or (B) *Mrp4* knockout mice. The bar graphs (bottom) show the averaged loop weight from (A) wild-type mice and (B) *Mrp4* knockout mice. The scale bar is 10 mm. Numbers in parentheses indicate the repeated times for each experimental condition. Error bars show SEM (n = 10–14). NS, no significance.

(C) The bar graphs showing the averaged loop weight injected with PBS with or without CTX (0.5 μg) from wild-type or *Mrp4* knockout mice. Data represent the mean ± SEM (n = 10–13).

(D) Representative mouse ileal loops 6 hr after luminal injection with CTX (0.5 μg) + MK571 (20 μM) with or without the CFTR-specific inhibitor, $CFTR_{inh}$-172 (20 μM), in wild-type mice.

secretion is mediated through the CFTR Cl^- channel because the CFTR-specific inhibitor, $CFTR_{inh}$-172, significantly inhibited fluid secretion (Figure 5D).

Cumulatively, our findings provide clear evidence that, (i) the potentiating effect on CTX-induced fluid secretion by MK571 is attributed to the inhibitory effect of MK571 on MRP4 transporter activity; and (ii) MRP4-deficient mice are more prone to CFTR-mediated secretory diarrhea. The latter argument is also supported by the MRP4 siRNA approach described above that is used to specifically knock down endogenous MRP4, followed by CFTR-mediated I_{sc} measurement (Figures 3B and S1C). The data from the intestinal fluid secretion study are consistent with the findings from the I_{sc} study, single-channel recordings, as well as the FRET-based intracellular cAMP dynamics described above.

A Macromolecular Complex of the MRP4 C-Tail and CFTR Is Mediated by PDZK1

Given that we observed a functional coupling between inhibition of MRP4 transporter activity and potentiation of CFTR Cl^- channel function, we next asked if a physical association between CFTR and MRP4 could be detected as well. Like CFTR, MRP4 possesses a consensus PDZ motif at its C terminus (-TAL_{COOH}). Therefore, it is possible that MRP4 can interact with PDZ proteins via a PDZ motif-based interaction. We therefore explored the binding affinity between MRP4 and several PDZ proteins that are reported to localize to the apical membrane of epithelial cells (Hung and Sheng, 2002; Li and Naren, 2005). Pull-down assays demonstrated that MRP4 binds to several PDZ proteins, and that it binds with the highest affinity to PDZK1 (Figure 6A). In order to quantify the binding affinity (EC_{50}) between MRP4 and PDZK1, two purified proteins were used in a binding kinetics study that demonstrated that MRP4 interacts with PDZK1 directly, with a binding constant of EC_{50} = 3.75 nM (Figure 6B).

We generated a polyclonal antibody against PDZK1 protein and detected expression of PDZK1 in both HT29-CL19A and T84 gut epithelial cells (Figure 6C). PDZK1 has been reported to interact with CFTR through a PDZ-based interaction (Wang et al., 2000). Given that both MRP4 and CFTR interact with PDZK1, and that these two transporters are colocalized to the apical membrane of gut epithelial cells (Figure 1D), we hypothesized that the interaction between MRP4 and CFTR was likely mediated by PDZK1. To address this, we assembled a macromolecular complex of the MRP4 C-tail, PDZK1, and CFTR in vitro, which is represented schematically in Figure 6D (top). A macromolecular complex was formed between the 50 C-terminal amino acids of MRP4, PDZK1, and CFTR (Figure 6D, bottom). The complex formation increased dose dependently with increasing amounts of the intermediary protein, PDZK1 (Figure 6D, bottom). We next immunoprecipitated CFTR from cultured gut epithelial cells that endogenously express all three proteins, and we demonstrated that both MRP4 and PDZK1 can be coimmunoprecipitated with CFTR (Figure 6E). These studies suggest that a macromolecular complex consisting of endogenous MRP4-PDZK1-CFTR is likely present on the apical surface of gut epithelial cells, and that it forms the basis for the functional coupling of MRP4 transporter activity to CFTR channel function that we observed in this study.

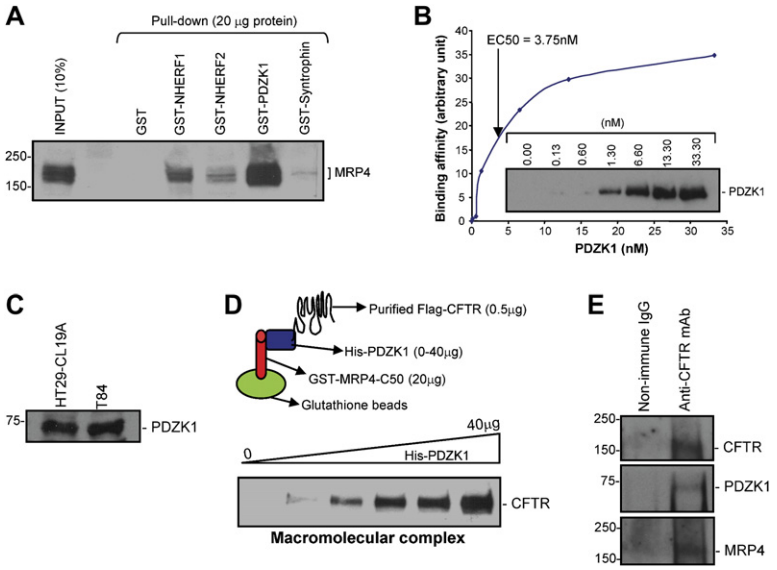

Figure 6. A Macromolecular Complex Is Formed between the MRP4 C-Tail, PDZK1, and CFTR

(A) MRP4 was pulled down by various GST-PDZ scaffolding proteins from lysates of HEK293 cells overexpressing MRP4.

(B) Binding of PDZK1 and 50 amino acids from the GST-MRP4 C-tail (EC_{50} = 3.75 nM). The inset shows a representative immunoblot of the dose-dependent interaction between His-PDZK1 and GST-MRP4-C50.

(C) PDZK1 expression in HT29-CL19A and T84 colonic epithelial cells by immunoblotting.

(D) A pictorial representation of the macromolecular complex assay (top; see Supplemental Experimental Procedures for details). A macromolecular complex was detected in vitro with three purified proteins (GST-MRP4-C50, His-PDZK1, and Flag-CFTR) in a dose-dependent manner.

(E) Cell lysates from HT29-CL19A cells were coimmunoprecipitated with anti-CFTR antibody (R1104) and probed for PDZK1 and MRP4. The MRP4 blot was visualized by using SuperSignal West Femto Maximum Sensitivity Substrate (Pierce) because of the weak signal.

Disrupting the Macromolecular Complex Inhibits the Functional Coupling between MRP4 and CFTR

To demonstrate the importance of a macromolecular complex containing MRP4, PDZK1, and CFTR in the MK571 potentiation of CFTR function, we disrupted the complex by using competitive MRP4 PDZ motif peptides (containing the last 10 amino acids, including the tripeptide PDZ motif at the extreme C terminus). We synthesized various peptides, with and without a biotin conjugate at the N terminus (MRP4-C10 WT), and mutant peptides with the alanine substitution point mutation of the last amino acid within the tripeptide PDZ motif (MRP4-C10-L1325A) (Figure 7A) and the alanine substitution mutations of the whole tripeptide PDZ motif (MRP4-C10-AAA) (Figure S6A). The biotin conjugate facilitated detection of the peptides with FITC-streptavidin. The competing efficacy of the peptides was confirmed by the pull-down in vitro binding studies, which showed that the synthetic wild-type peptides substantially competed with the GST fusion protein of the 50 C-terminal amino acids of MRP4 for binding to PDZK1 (Figures 7A and S6A) compared to the controls. The mutant peptides demonstrated significantly less efficacy of competition (Figures 7A and S6A). This clearly shows that the tripeptide PDZ motif (-TAL_{COOH}) at the extreme C terminus of a MRP4 transporter is critical for the physical interaction between MRP4 and PDZK1. Using a high-efficient peptide delivery system (Chariot system; see Li et al., 2005), we delivered these peptides into polarized gut epithelial cells before I_{sc} measurements stimulated by ADO. Our data clearly demonstrates that the MRP4-specific peptides significantly attenuated the MK571-elicited potentiation of CFTR-mediated currents in gut epithelial cells (Figure 7B). At the end of the experiment, the epithelial cells were fixed and immunostained with FITC-streptavidin to confirm that the peptide was delivered into the cells (Figure 7C, right).

To rule out the possibility that the MRP4 peptides might interfere with other PDZ domain interaction (or these peptides might inhibit PDZK1 interactions with other target proteins), and to confirm that MRP4 peptide does disrupt the local macromolecular complex in these peptide-delivered epithelial cells, we also performed the coimmunoprecipitation with PDZK1 antibody. The coimmunoprecipitated CFTR and MRP4 amounts were checked by immunoblotting. As the data showed, MRP4 wild-type peptide significantly reduced the endogenous MRP4 protein amount that was coimmunoprecipitated with PDZK1 in HT29-CL19A epithelial cells (Figure S6B, right). However, MRP4 wild-type peptide did not affect the CFTR amount coimmunoprecipitated with PDZK1 (Figure S6B, left), which suggests the specificity of the MRP4 peptide. MRP4-L1325A mutant peptide behaved in a similar fashion to the biotin control (Figure S6B).

DISCUSSION

Secretory epithelia perform vectorial transport of salt and water molecules by coordinated actions of the transporters expressed in polarized epithelial membranes, and CFTR is one of the key membrane proteins regulating overall fluid movements. Hypo- or hyperfunctioning of CFTR can cause aberrant membrane transport and may result in life-threatening diseases, such as cystic fibrosis or secretory diarrhea (Kunzelmann and Mall, 2002). Therefore, the fine-tuned regulation of salt and water transport is essential in epithelial and body homeostasis.

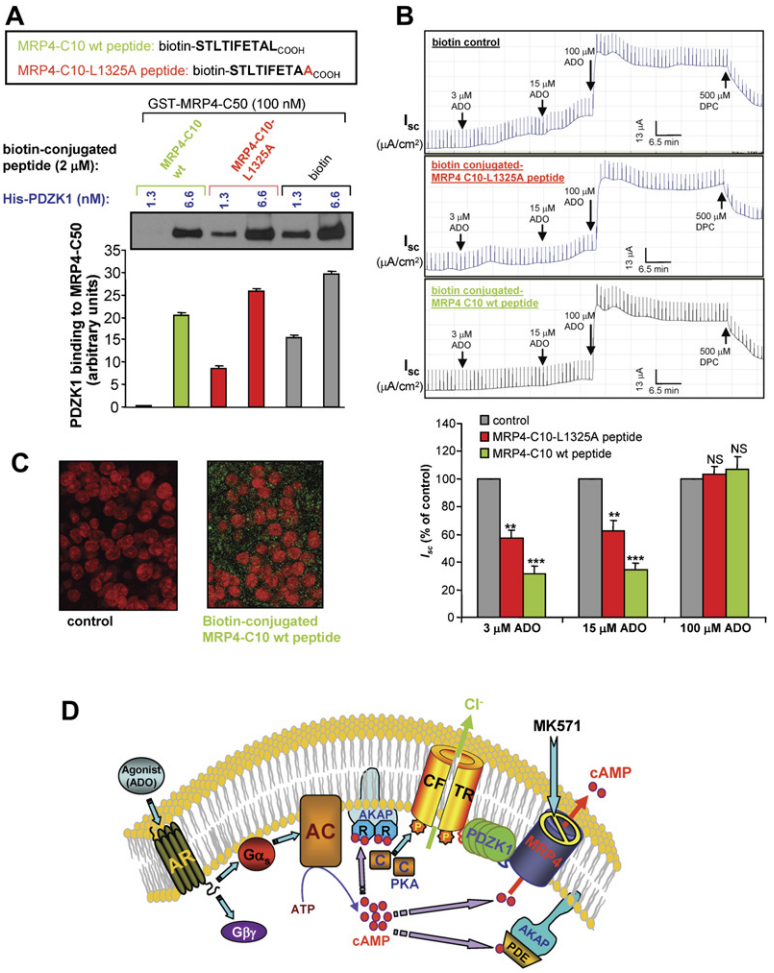

Figure 7. MRP4 Peptides that Disrupt MRP4 Interaction with PDZK1 Attenuate Elevation of CFTR Cl⁻ Currents Mediated by MRP4 Inhibition

(A) PDZK1 binding to MRP4 in the presence of biotin-conjugated MRP4 C-tail peptides (last 10 amino acids; wild-type and mutant L1325A). The bar graphs (bottom) show the averaged band density from respective groups. Data represent the mean ± SEM (n = 3).

(B) Representative short-circuit current (I_{sc}) traces in response to ADO in HT29-CL19A-polarized cells. MRP4 peptides (2 μM) were delivered to the cells before I_{sc} measurement. Cells in all groups were pretreated with 20 μM MK571 for 30 min before activation with ADO. Bar graphs summarize the averaged maximal I_{sc} after each dose of ADO as a percentage of the control. Results are presented as mean ± SEM (n = 3–4 for each group). NS, no significance; **p < 0.01; ***p < 0.001 compared with the control for each ADO dose.

(C) Immunofluorescence micrographs of HT29-CL19A cells from (B) showing the biotin-conjugated MRP4 peptides (green; right) delivered into the polarized cells. The nucleus was stained with propidium iodide (red). FITC-streptavidin was used to detect the biotin conjugated with the peptides.

(D) Schematic representation of the compartmentalized signaling involved in the spatiotemporal coupling of cAMP transporter (MRP4) to the CFTR Cl⁻ channel in the gut epithelia. Refer to the Discussion for details.

Spatiotemporal Coupling of cAMP Transporter Function and CFTR Cl⁻ Channel Activity

In the present study, we found that inhibition of a cAMP transporter, MRP4, by MK571 potentiated CFTR-mediated Cl⁻ currents. We also observed that potentiation of CFTR function by MK571 was most prominent when CFTR was activated by lower concentrations of ADO (<20 μM), but not with higher doses of agonists (>20 μM). This suggests that lower doses of ADO may lead to compartmentalized cAMP accumulation, which is further enhanced by the reduced or inhibited cAMP efflux through MRP4 by MK571. This finding is consistent with the previous observation that cAMP is generated in a compartmentalized pocket upon stimulation by 2 μM ADO, which is enough to activate CFTR function in the proximity, and that LPA, a cAMP-lowering agent, significantly inhibits CFTR function (Li et al., 2005). Here, the concept of cAMP compartmentalization was recapitulated with the treatment of MK571, which significantly potentiated CFTR function when it was stimulated by lower doses of ADO. It has been reported that inhibiting the transport of MRP4 does not lead to substantial increases of intracellular cyclic nucleotide levels (globally); neither does overexpression of MRP4 lead to a substantial decrease in intracellular cAMP levels, even when these levels are high (Wielinga et al., 2003). This is probably because the inhibition of MRP4 resulted only in localized fluctuations of cyclic nucleotide levels, but not global levels.

Based on previous findings and the data obtained from this study, we propose a model depicting the spatiotemporal coupling of cAMP transporter to CFTR Cl⁻ channel function in the gut epithelia (Figure 7D). Underneath the apical plasma membrane, highly localized compartments exist and contain a series of signaling molecules such as AR; G protein (Gs); AC; PKA and its anchoring proteins, AKAPs; CFTR; cAMP transporter (MRP4); and PDZ scaffolding proteins (in this case, PDZK1). PDZK1 functions to physically connect CFTR to MRP4. This macromolecular signaling complex provides a potential anatomical basis for the generation and modulation of local cAMP compartments. When an agonist (in this case, ADO) binds AR, a series of G protein-mediated reactions leads to the activation of AC present in the apical membrane. Sufficient cAMP (red spheres; Figure 7D) is locally generated in a diffusionally restricted apical microdomain (but not in other cellular compartments). cAMP activates PKA,

which is also anchored to the apical membrane by AKAP (i.e., ezrin), and phosphorylates the CFTR Cl^- channel in the close vicinity, resulting in an increase of Cl^- currents. The CFTR-mediated Cl^- currents can be further increased (potentiated) through the additional increase of local cAMP resulting from the reduced or blocked efflux via a neighboring apical membrane cAMP transporter (MRP4) in the same subcellular compartment.

In general, it is believed that PDEs provide the sole means for degrading cAMP in cells and play a vital role in shaping intracellular gradients of the second messenger (Cooper, 2005; Jackson and Raghvendra, 2004). Here, we identified additional means of regulating cAMP levels in a microdomain underneath the surface membrane, an efflux path for cAMP via the MRP4 transporter in the close vicinity of the CFTR-containing signaling complex. The interaction between CFTR and MRP4 provides an additional layer of mechanism to regulate CFTR function, which is important in maintaining epithelial and body homeostasis.

Macromolecular Signaling Complex in the Gut

PDZ domains are conserved protein-interaction modules that are ~80–90 amino acids long, fold to form peptide-binding clefts, and typically mediate interactions with the carboxyl termini of target proteins that terminate in consensus PDZ-binding sequences (i.e., PDZ motif) (Hung and Sheng, 2002; Li and Naren, 2005). PDZK1 has been reported to interact with CFTR, SLC26A3 (downregulated in adenoma [DRA]), SLC26A6 (putative anion transporter 1 [PAT1]), and the Na^+/H^- exchanger NHE3, the major transport proteins for intestinal anion secretion and salt absorption (Lamprecht and Seidler, 2006). Many studies have reported the association of these PDZ proteins with a wide variety of ion channels, receptors, transporters, and signaling proteins on the apical surfaces of cells, suggesting that apical membrane PDZ proteins could facilitate the formation of multiprotein complexes clustered within microdomains that modulate trafficking, transport, and signaling in polarized epithelial cells (Wang et al., 2000; Lamprecht and Seidler, 2006).

Compartmentalization of signaling complexes containing CFTR, PDZK1, and MRP4 (Figure 7D) has important implications. Our present study demonstrates a physically and functionally interacting macromolecular complex containing two ABC transporters mediated by a PDZ scaffolding protein, which may have significant in vivo physiological or pathophysiological relevance. Under normal conditions, MRP4 pumps out cAMP, which is in proximity to CFTR, thus modulating CFTR function stimulated by cAMP-producing pathways (such as ADO). Under aberrant conditions (such as inflammatory bowel disease with diarrhea or irritable bowel syndrome with constipation), the expression levels and/or subcellular localization of CFTR and/or MRP4 may be dysregulated. The ratio of CFTR to MRP4 may be altered, thereby resulting in elevated or reduced cAMP accumulation in the compartment and leading to enhanced or attenuated CFTR-mediated Cl^- transport, which consequently results in secretory diarrhea in inflammatory bowel disease or constipation occurring in irritable bowel syndrome. In inflamed colonic mucosa of mice with inflammatory bowel disease, CFTR expression was increased 2.5-fold compared to noninflamed samples (Lohi et al., 2002). Elevated CFTR expression and enhanced cAMP-dependent Cl^- secretion have been demonstrated in hyperproliferated mouse intestine (Umar et al., 2000). In *Cftr* knockout mice, ileal mucosal bile acid absorption is increased significantly compared to wild-type mice (Stelzner et al., 2001). Interestingly, MRP4 is reported to be an alternative bile acid export pump (Rius et al., 2003). This suggests a possible upregulation of MRP4 function in the absence of CFTR. Our present studies have significant in vivo implications for diseases such as secretory diarrhea, inflammatory bowel disease, and irritable bowel syndrome.

EXPERIMENTAL PROCEDURES

Short-Circuit Current Measurements

Polarized colonic epithelial cells (HT29-CL19A and T84) were grown to confluency on permeable supports before they were mounted in a Ussing chamber, and short-circuit currents (I_{sc}) were measured as reported previously (Li et al., 2005). MK571 (5–50 μM) was added to both the apical and basolateral sides for 30 min before ADO was added to the apical side. In some experiments, cells were permeabilized at the basolateral side with 100 μg/ml α-toxin for 30 min at 37°C before the I_{sc} measurement was taken. The CFTR inhibitor DPC (500 μM), glybenclamide (500 μM), or $CFTR_{inh}$-172 (2–10 μM) was added onto the apical side.

[^{3}H]cAMP and Etheno-cAMP Transport Assay across Apical Cell Membranes

HT29-CL19A and T84 cells were permeabilized at the basolateral side with α-toxin as described above, and they were incubated with MK571 or PMEA at 37°C for 30 min. [^{3}H]cAMP or etheno-cAMP was added into the basolateral chamber containing 4 mM ATP (Mg salt). For the [^{3}H]cAMP transport assay, an aliquot of 40 μl apical solution was collected at various time points, and the radioactivity was measured with a liquid scintillation counter (LS5000TA; Beckman Coulter, Fullerton, CA). For the etheno-cAMP transport assay, an aliquot of 40 μl apical solution was collected, and the fluorescence was measured at wavelength ex315 nm/em420 nm with a fluorescence spectrophotometer (F-2500; Hitachi, Tokyo, Japan).

Coimmunoprecipitation and Immunoblotting

Cells were harvested and processed for coimmunoprecipitation and immunoblot as described previously (Li et al., 2005). Cells were solubilized in RIPA buffer for immunoblot alone or in PBS-0.2% Triton X-100 for coimmunoprecipitation, and lysates were spun at 15,000 × g for 15 min at 4°C to pellet insoluble material and processed for coimmunoprecipitation and immunoblot as described in detail in Supplemental Experimental Procedures.

Cell-Attached Single-Channel Recordings

Single-channel recordings were obtained from HT29-CL19A cells as reported previously (Li et al., 2005). CFTR channels were activated with adenosine (0–40 μM) included in the pipette as indicated. Single-channel currents were continuously recorded for 5 min at a test potential of +100 mV (referenced to the cell interior) delivered from the recording electrode and were filtered at 1 kHz and sampled at 2 kHz (Li et al., 2005; details in Supplemental Experimental Procedures).

FRET Imaging Microscopy and Image Analysis

Cells (expressing CFP-EPAC-YFP) for FRET imaging were seeded in 35 mm glass-bottom dishes (MatTek) and were grown for 24–48 hr and washed with HBSS before being mounted on an Olympus microscopy system for FRET imaging. Images were recorded with a cooled CCD Hamamatsu ORCA285 camera (Hamamatsu, Japan) mounted on the Olympus microscope IX51 (U-Plan Fluorite 60 × 1.25 NA oil-immersion objective), and the system was controlled by SlideBook 4.1 software (Intelligent Imaging Innovations, Denver, CO); ratio and FRET modules were used to obtain and analyze the images. Excitation light was provided by a 300W Xenon lamp and was attenuated with a ND filter with 50% light transmission. Images were captured by using a JP4 CFP/YFP filter set (Chroma, Brattleboro, VT) including a 430/25 nm excitation filter, a double dichroic beam splitter, and two emission filters (470/30 nm for CFP and 535/30 nm for FRET) alternated by a filter-changer Lambda 10-3 (Sutter Instruments, Novato, CA). Time-lapse images were acquired with a 4 × 4 binning mode, a 200–400 ms exposure time, and 1 min intervals to reduce photobleaching of the fluorophores. Acquired fluorescent images were background subtracted, and multiple regions of interest (ROIs) on the cell periphery were selected for quantitative data analysis (~20–30 ROIs per cell, and 4–6 cells per condition were averaged). The emission ratio images (CFP/FRET) were generated at different time points on a pixel-by-pixel basis by the SlideBook ratio module as formulated below,

$$R = \frac{\text{Emission intensity of background-subtracted CFP image}}{\text{Emission intensity of background-subtracted FRET image}}. \quad (1)$$

The ratio (R) was normalized as R_t/R_0, where R_t is the ratio at time point t and R_0 is the ratio at time point 0 (just before the addition of the first test compound). The cell images are presented in pseudocolor to highlight the changes in the ratio of CFP/FRET fluorescence intensity.

Macromolecular Complex Assembly

The in vitro complex formation (Li et al., 2005) was performed by mixing GST-His-S-MRP4-C terminal 50 aa fusion protein (20 μg) with various amounts of His-S-PDZK1 (0–40 μg) and 0.5 μg purified Flag-tagged WT-CFTR at 4°C for 3 hr (Li et al., 2005; details in Supplemental Experimental Procedures).

MRP4 Peptide In Vitro Competitive Binding

MRP4 peptides (biotin-conjugated wild-type or L1325A mutant peptide, or nonconjugated wild-type or C10-AAA mutant peptide; 2 μM each) were mixed with His-PDZK1 (1.3 and 6.6 nM) at 22°C–24°C for 1 hr before GST-MRP4-C50 (immobilized on glutathione beads) was added; the solution was then mixed for another hour. The beads were washed, and the protein complex was eluted from the beads, separated by SDS-PAGE, and immunoblotted with rabbit anti-PDZK1 polyclonal antibody as described above.

Delivery of MRP4 Peptide into Polarized Epithelial Cells, followed by Immunocytochemistry and Coimmunoprecipitation

Delivery of MRP4-specific peptide was performed as reported before (Li et al., 2005) and is described in detail in Supplemental Experimental Procedures. After I_{sc} measurement, the cells were fixed and immunostained for the peptides by using FITC-conjugated streptavidin. In some experiments, after peptide delivery and I_{sc} measurement, cells in the filters were scraped into RIPA buffer, and coimmunoprecipitation with rabbit PDZK1 antibody was performed. Endogenous CFTR and MRP4 protein amounts in the coimmunoprecipitated complex were checked by immunoblotting with anti-CFTR (R1104 monoclonal) and anti-MRP4 (M_4I-10, rat monoclonal) antibodies as described above.

MRP4 siRNA to Knock Down MRP4 in Polarized Epithelial Cells

MRP4 siRNA and Lipofectamine 2000 transfection reagent were prepared and mixed according to the manufacturer's instructions. siRNA-Lipofectamine 2000 complexes were added to HT29-CL19A cells grown to confluency on transwells and were incubated at 37°C in a CO_2 incubator. After 60–72 hr, the transwells were mounted in a Ussing chamber for I_{sc} measurement in response to ADO stimulation. After the Ussing chamber study, the transwells were washed with PBS, and the cells were scraped into RIPA lysis buffer. The protein levels of MRP4, CFTR, and PDZK1 were assessed by western blot with corresponding antibodies.

Statistical Analysis

Results are presented as mean ± SEM for the indicated number of experiments. Statistical analysis was performed by using a Student's t test and one-way ANOVA. A value of $p < 0.05$, $p < 0.01$, or $p < 0.001$ was considered statistically significant.

Supplemental Data

Supplemental Data include Supplemental Experimental Procedures, Supplemental References, and six figures and can be found with this article online at http://www.cell.org/cgi/content/full/131/5/940/DC1/.

ACKNOWLEDGMENTS

We thank Dr. David Armbruster for critically reading the manuscript and Ms. Lillian Zalduondo for kind assistance with mice ileal loop experiments. We also thank Dr. Gabor Tigyi for help in obtaining constructs, Dr. Rick Heil-Chapdelaine for FRET imaging support, and Danny Morse for graphics. This work was supported by grants from the National Institutes of Health (to A.P.N., J.D.S., and D.J.N.), American Lebanese Syrian Associated Charities (to J.D.S.), the American Lung Association (to A.P.N.), and the American Heart Association - Greater Southeast Affiliate (#0765185B to C.L.).

Received: May 3, 2007
Revised: July 17, 2007
Accepted: September 13, 2007
Published: November 29, 2007

REFERENCES

Barrett, K.E., and Keely, S.J. (2000). Chloride secretion by the intestinal epithelium: molecular basis and regulatory aspects. Annu. Rev. Physiol. *62*, 535–572.

Chen, Z.S., Lee, K., and Kruh, G.D. (2001). Transport of cyclic nucleotides and estradiol 17-β-D-glucuronide by multidrug resistance protein 4. Resistance to 6-mercaptopurine and 6-thioguanine. J. Biol. Chem. *276*, 33747–33754.

Clarke, L.L., Grubb, B.R., Gabriel, S.E., Smithies, O., Koller, B.H., and Boucher, R.C. (1992). Defective epithelial chloride transport in a gene targeted mouse model of cystic fibrosis. Science *257*, 1125–1128.

Cooper, D.M. (2005). Compartmentalization of adenylate cyclase and cAMP signalling. Biochem. Soc. Trans. *33*, 1319–1322.

Davare, M.A., Avdonin, V., Hall, D.D., Peden, E.M., Burette, A., Weinberg, R.J., Horne, M.C., Hoshi, T., and Hell, J.W. (2001). A β2 adrenergic receptor signaling complex assembled with the Ca^{2+} channel Cav1.2. Science *293*, 98–101.

Dean, M., Rzhetsky, A., and Allikmets, R. (2001). The human ATP-binding cassette (ABC) transporter superfamily. Genome Res. *11*, 1156–1166.

Hasko, G., and Cronstein, B.N. (2004). Adenosine: an endogenous regulator of innate immunity. Trends Immunol. *25*, 33–39.

Huang, P., Lazarowski, E.R., Tarran, R., Milgram, S.L., Boucher, R.C., and Stutts, M.J. (2001). Compartmentalized autocrine signaling to cystic fibrosis transmembrane conductance regulator at the apical membrane of airway epithelial cells. Proc. Natl. Acad. Sci. USA *98*, 14120–14125.

Hung, A.Y., and Sheng, M. (2002). PDZ domains: structural modules for protein complex assembly. J. Biol. Chem. *277*, 5699–5702.

Jackson, E.K., and Raghvendra, D.K. (2004). The extracellular cyclic AMP-adenosine pathway in renal physiology. Annu. Rev. Physiol. *66*, 571–599.

Kunzelmann, K., and Mall, M. (2002). Electrolyte transport in the mammalian colon: mechanisms and implications for disease. Physiol. Rev. *82*, 245–289.

Lai, L., and Tan, T.M. (2002). Role of glutathione in the multidrug resistance protein 4 (MRP4/ABCC4)-mediated efflux of cAMP and resistance to purine analogues. Biochem. J. *361*, 497–503.

Lamprecht, G., and Seidler, U. (2006). The emerging role of PDZ adapter proteins for regulation of intestinal ion transport. Am. J. Physiol. Gastrointest. Liver Physiol. *291*, G766–G777.

Li, C., and Naren, A.P. (2005). Macromolecular complexes of cystic fibrosis transmembrane conductance regulator and its interacting partners. Pharmacol. Ther. *108*, 208–223.

Li, C., Dandridge, K.S., Di, A., Marrs, K.L., Harris, E.L., Roy, K., Jackson, J.S., Makarova, N.V., Fujiwara, Y., Farrar, P.L., et al. (2005). Lysophosphatidic acid inhibits cholera toxin-induced secretory diarrhea through CFTR-dependent protein interactions. J. Exp. Med. *202*, 975–986.

Lohi, H., Makela, S., Pulkkinen, K., Hoglund, P., Karjalainen-Lindsberg, M.L., Puolakkainen, P., and Kere, J. (2002). Upregulation of CFTR expression but not SLC26A3 and SLC9A3 in ulcerative colitis. Am. J. Physiol. Gastrointest. Liver Physiol. *283*, G567–G575.

Naren, A.P., Cobb, B., Li, C., Roy, K., Nelson, D., Heda, G.D., Liao, J., Kirk, K.L., Sorscher, E.J., Hanrahan, J., and Clancy, J.P. (2003). A macromolecular complex of β2 adrenergic receptor, CFTR, and ezrin/radixin/moesin-binding phosphoprotein 50 is regulated by PKA. Proc. Natl. Acad. Sci. USA. *100*, 342–346.

Ponsioen, B., Zhao, J., Riedl, J., Zwartkruis, F., van der Krogt, G., Zaccolo, M., Moolenaar, W.H., Bos, J.L., and Jalink, K. (2004). Detecting cAMP-induced Epac activation by fluorescence resonance energy transfer: Epac as a novel cAMP indicator. EMBO Rep. *5*, 1176–1180.

Reddy, M.M., and Quinton, P.M. (1996). Deactivation of CFTR GCl by endogenous phosphatases in the native sweat duct. Am. J. Physiol. *270*, C474–C480.

Reid, G., Wielinga, P., Zelcer, N., De Haas, M., Van Deemter, L., Wijnholds, J., Balzarini, J., and Borst, P. (2003). Characterization of the transport of nucleoside analog drugs by the human multidrug resistance proteins MRP4 and MRP5. Mol. Pharmacol. *63*, 1094–1103.

Rius, M., Nies, A.T., Hummel-Eisenbeiss, J., Jedlitschky, G., and Keppler, D. (2003). Cotransport of reduced glutathione with bile salts by MRP4 (ABCC4) localized to the basolateral hepatocyte membrane. Hepatology *38*, 374–384.

Schuetz, J.D., Connelly, M.C., Sun, D., Paibir, S.G., Flynn, P.M., Srinivas, R.V., Kumar, A., and Fridland, A. (1999). MRP4: a previously unidentified factor in resistance to nucleoside-based antiviral drugs. Nat. Med. *5*, 1048–1051.

Steinberg, S.F., and Brunton, L.L. (2001). Compartmentation of G protein-coupled signaling pathways in cardiac myocytes. Annu. Rev. Pharmacol. Toxicol. *41*, 751–773.

Stelzner, M., Somasundaram, S., Lee, S.P., and Kuver, R. (2001). Ileal mucosal bile acid absorption is increased in Cftr knockout mice. BMC Gastroenterol. *1*, 10–16.

Umar, S., Scott, J., Sellin, J.H., Dubinsky, W.P., and Morris, A.P. (2000). Murine colonic mucosa hyperproliferation. I. Elevated CFTR expression and enhanced cAMP-dependent Cl^- secretion. Am. J. Physiol. Gastrointest. Liver Physiol. *278*, G753–G764.

van Aubel, R.A., Smeets, P.H., Peters, J.G., Bindels, R.J., and Russel, F.G. (2002). The MRP4/ABCC4 gene encodes a novel apical organic anion transporter in human kidney proximal tubules: putative efflux pump for urinary cAMP and cGMP. J. Am. Soc. Nephrol. *13*, 595–603.

Wang, S., Yue, H., Derin, R.B., Guggino, W.B., and Li, M. (2000). Accessory protein facilitated CFTR-CFTR interaction, a molecular mechanism to potentiate the chloride channel activity. Cell *103*, 169–179.

Wielinga, P.R., van der Heijden, I., Reid, G., Beijnen, J.H., Wijnholds, J., and Borst, P. (2003). Characterization of the MRP4- and MRP5-mediated transport of cyclic nucleotides from intact cells. J. Biol. Chem. *278*, 17664–17671.